Spectral performance and effect of spatial-energetic correlation in PCD with different converter materials

Xiaoqing Li[*1], Paurakh L. Rajbhandary[2], Jinghui Wang[2], Mats Persson[2],Zhifang Wu[1], Norbert J. Pelc[2]
*l). Institute of Nuclear and New Energy Technology ,Tsinghua University, Beijing, 100084,li-xq15@mails.tsinghua.edu.cn
2).Departments of Bioengineering and Radiology, Stanford University, Stanford, CA,94305

Photon counting detectors (PCD) are promising as next generation detectors for spectral imaging applications. Sensors based on cadmium telluride (CdTe) and silicon (Si) are already in experimental use and sensors based on gallium arsenide (GaAs) , a promising material for PCDs are being researched[1]. These materials suffer from different undesirable phenomena such as escape of Compton scatter, fluorescence escape and charge sharing. These events can result in multi-counting of a single incident photon in neighbor pixels. Accurately modeling these effects can be crucial for detector design and for model based correction. In this paper, we derive an accurate model for multi-counting events and correlations to compare the expected performance of CdTe, GaAs and Si. Detectors based on these materials differ in their structure in their practical use. CdTe is used face-on and is on the order of 3mm in thickness. We simulate the correlations in a 3×3 pixel grid, with each pixel being 500×500 μm^2. GaAs and Si need to be much thicker and are oriented edge-on in our simulation. We use a 6cm deep structure for Si and 1 cm for GaAs, again with each pixel being 500×500 μm^2. Mean and covariance matrices are deduced using spatio-energy functions estimated from Monte Carlo simulation and a material-specific, energy-independent spherical charge cloud model (give the radii for the three materials). Then we use the Cramer-Rao lower bound (CRLB) to estimate the variance of the estimated basis material thicknesses for the three detectors.

Keywords—Photon counting detectors; spatio-energetic correlation; converter materials

I. PURPOSE

Photon counting detectors are able to provide energy-discrimination and promise several advantages. However, effect of imperfect energy response and spatial-energetic correlation due to scattering, charge sharing and fluorescence escape degrades PCD measurements. Of the two widely used converter materials: Si has lots of Compton scatter while CdTe has less scatter but has higher K-binding energies(Cd at 26.7keV and Te at 31.81keV) and associated escape of fluorescence x-rays, both phenomena degrade the detector performance. As to GaAs, the K-binding energy is about 10keV and its Compton scatter is also in-between the other two materials. So, we chose these three materials to study to suggest properties of an ideal material. Taguchi[2] proposed a deterministic method to estimate correlation in PCDs and applied it to *3×3* pixel grid but did not study the impact of double counting. In this paper, we will use a model that consider multi-counting. We also calculate the radius of charge sharing to improve our method and we use the improved method to study the effect of correlation and multi-counting in the three detector converter materials: CdTe, GaAs and Si.

II. METHODS

A. Detector models

In practical use, the structure of detectors of the different materials can be different. Figure 1 shows our structures for CdTe, GaAs and Si. Figure 1 (a) shows the CdTe detector, which is face-on, with x-rays incident in the x-y plane. We set the detector thickness to be 3mm with a z-directed electric field created by 1000V applied along the z-axis.

GaAs and Si are edge-on; a single detector strip is shown in figure 1 (b) but an actual detector would have many strips along the y direction. X-rays are incident in the x-y plane. GaAs is assumed to be 1 cm thick and Si is 6cm thick along the z-direction. The lateral cell size is 0.5mm with a y-directed electric field created by 300V applied along the y-axis.

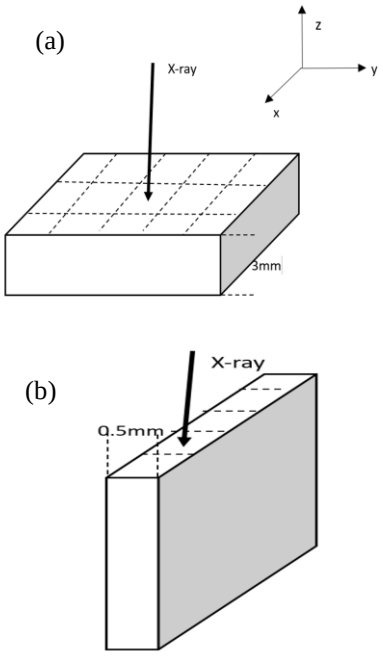

Figure 1 . structure of CdTe (a), modality of GaAs and Si (b)

B. *Spatio-energy model*

To examine the effect of spatio-energetic correlation and to evaluate the low spatial frequency performance, we simulate a setting in which a uniform object covers a 3x3 pixel grid. Since we are evaluating the low spatial frequency performance, we assume the signals from all 9 pixels are used to estimate the object composition. For comparison, we also simulate illumination of the single central detector pixel.

There are differences between detectors made from CdTe and the other two materials. In CdTe (shown in Figure 2(a)), because it is face-on, we consider escaped photons and charge sharing of all the pixels in both x-axis and y-axis. In Si and GaAs (shown in Figure 2(b)), because they are edge-on, we consider escaped photons of all pixels but only consider charge sharing along the x-axis.

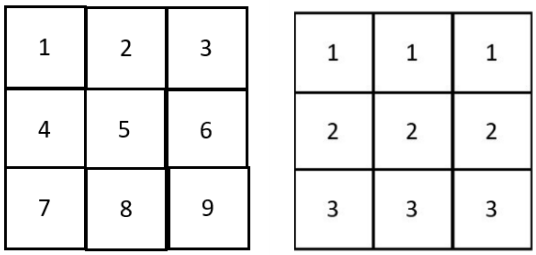

(a) (b)

Figure 2. pixel grid for CdTe (a), GaAs and Si (b)

C. *Charge sharing*

We consider charge sharing due to collection of the electron cloud. The charge cloud radius depends on the applied voltage, photon energy and the thickness of detector. We simplify the charge cloud modeling by using these assumptions:

1. We suppose the charge cloud is an isotropic sphere of uniformly distributed charge.
2. The original size of the charge cloud is very small, so we assume it to be zero .
3. We only consider diffusion, and ignore the Coulombian force during charge diffusion.

The radius of the charge cloud increases with increasing distance of diffusion, which is the distance from the photon absorption to the electrodes. We use the mean absoption distance to calculate the CdTe charge cloud. Since the GaAs and Si are edge-on, we assume a photon incident on the x-axis. The radius of the charge cloud is also related to the electric field. CdTe and GaAs both have a uniform electric field whereas Si is like a PIN diode and the way to calculate its electric field is different from the other materials.

Our result showed that the radius of the CdTe charge cloud is about 60μm, that of GaAs is about 14μm and Si is about 12μm. These results are reasonable compared with the literature. In our simulations we assumed this size charge cloud for all photons.

D. *Spatio-energy response function(SERF)[3]:*

The Spatio-Energy Response Functions (SERF) reflect the energy response of the detector pixels and the correlation between one pixel and the neighboring pixels(Figure 3) with 1keV energy sampling. It is deduced using Monte Carlo simulation using pyPENELOPE[4]. We use the symbols listed below :

— SERF(i,i)(E1, E') gives fraction of photon with incident energy E' that deposit energy E1 in the central pixel i.

— SERF(i,j)(E1, E2, E') gives fraction of photons with incident energy E' that deposit energy E1 in the central i pixel and energy E2 in the neighboring pixel .j

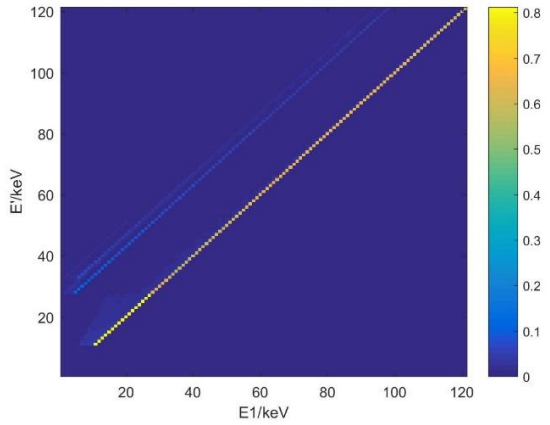

(a)

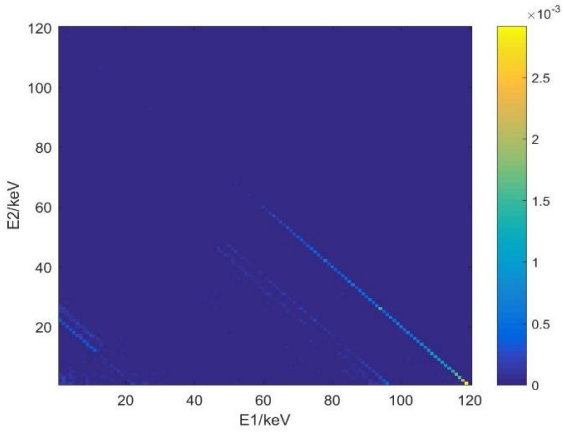

(b)

Figure 3: (a) $SERF_{(i,i)}(E_1, E')$ shows fraction of photons with incident energy E' and deposit energy E_1 in the central pixel i. (b) $SERF_{(i,j)}(E_1, E_2, E')$ gives fraction of photons with incident energy E' that deposit energy E_1 in the central pixel i and energy E_2 in the neighboring pixel j.

Our simulation did not include the effects of electronic noise. From the spatio-energy response function, we can get the spectrum of the counts measured in the incident pixel and in the neighboring pixels. Figure 4 shows such spectra for monoenergetic 120 keV photon

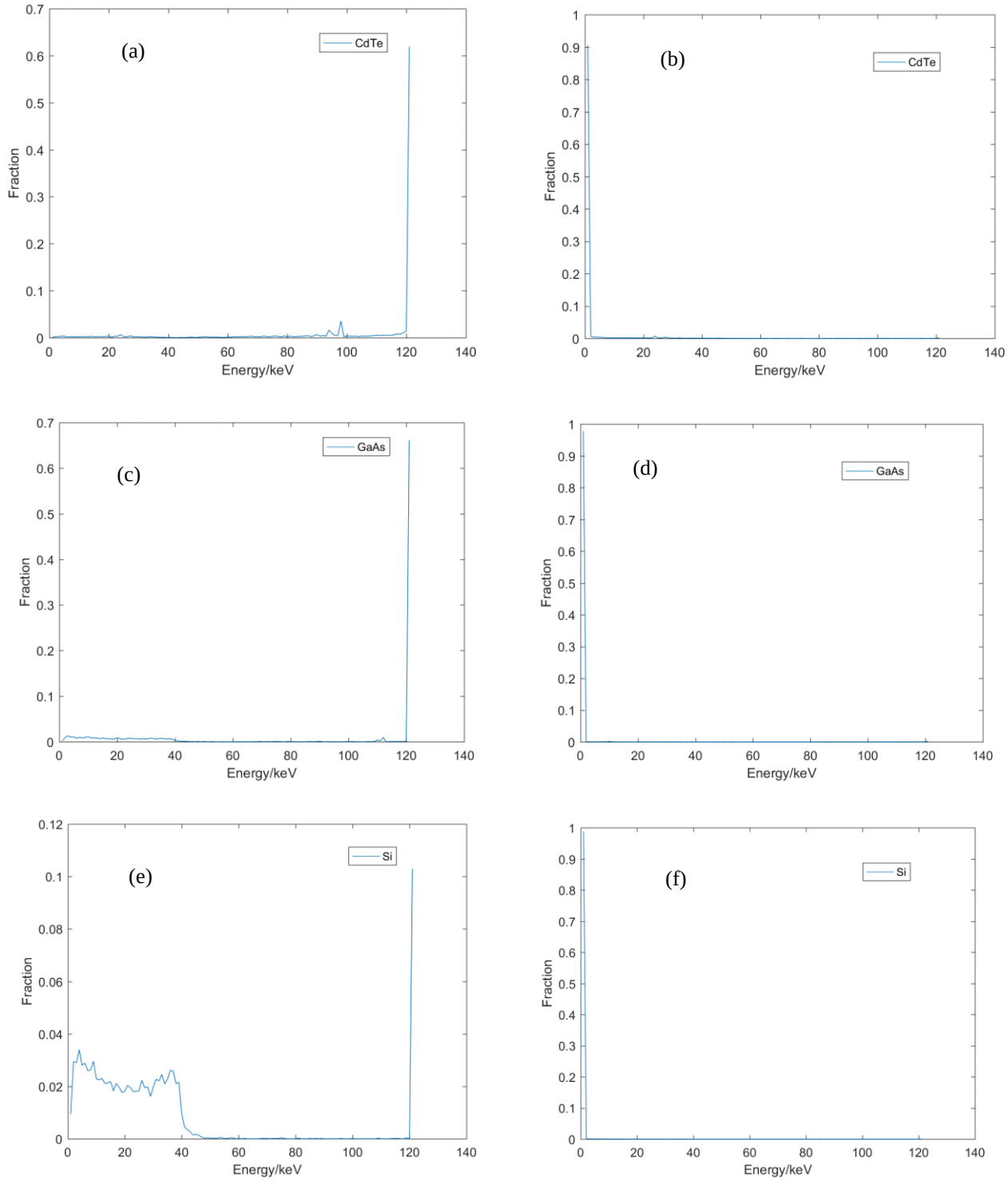

Figure 4: (a)shows the spectrum of CdTe in central pixel with incident energy 120keV. (b)shows the spectrum of CdTe in abutting pixel with incident energy 120keV. (c)shows the spectrum of GsAs in central pixel with incident energy 120keV. (d)shows the spectrum of GaAs in abutting pixel with incident energy 120keV. (e)shows the spectrum of Si in central pixel with incident energy 120keV. (f)shows the spectrum of Si in abutting pixel with incident energy 120keV.

E. Spatio-Energetic Correlation of a 3x3 Pixel Grid:

After grouping of counts into energy bins the covariance matrix Σ is:

$$\Sigma_{I_i[i]\times I_j[j]} = \begin{bmatrix} \sum_{E'=1}^{E_{max}} I(E') \quad SERF_{(i,i)}(E,E')^T \times \sqcap_{E_l{}^i}^{E_h{}^i}(E) & \sum_{E'=1}^{E_{max}} \sum_{E_1=E_l{}^i}^{E_h{}^i} \sum_{E_2=E_l{}^j}^{E_h{}^j} [SERF_{(i,j)}(E_1,E_2,E') \; I(E')] \\ \sum_{E'=1}^{E_{max}} \sum_{E_1=E_l{}^i}^{E_h{}^i} \sum_{E_2=E_l{}^j}^{E_h{}^j} [SERF_{(i,j)}(E_1,E_2,E') \; I(E')] & \sum_{E'=1}^{E_{max}} \sum_{E_1=1}^{E_{max}} \sum_{E_2=E_l{}^j}^{E_h{}^j} [SERF_{(i,j)}(E_1,E_2,E') \; I(E')] \end{bmatrix} \quad (1)$$

where,

$E_l{}^i$ & $E_h{}^i$ are low and high threshold of energy bin "i"

$E_l{}^j$ & $E_h{}^j$ are low and high threshold of energy bin "j"

$$\sqcap_{E_l}^{E_h{}^i}(E) \in \mathbb{R} = \begin{cases} 1, & E_l{}^i < E < E_h{}^i \\ 0, & otherwise \end{cases},$$

When all nine pixels of a 3×3 pixel grid are uniformly illuminated, superposition of corresponding elements of $\Sigma I_{(i,i)}[i]\times I_{(i,j)}[j]$ can be used to derive 9N×9N spatio-covariance matrix, where N is the number of energy bins.

F. CRLB calculations

As a surrogate of the low spatial frequency response, after getting the spatio-covariance matrix, we calculate the mean counts μ and covariance matrix Σ of macro-pixels for different detector materials. We numerically estimate the derivative of the mean with respect to the two basis material components for spectral measurements. The Fisher information matrix F[5] is then estimated using:.

$$\mathcal{F}_{ij} = \left[\frac{\partial \mu(\boldsymbol{m})}{\partial m_i}\right]^T \Sigma^{-1}(\boldsymbol{m}) \left[\frac{\partial \mu(\boldsymbol{m})}{\partial m_j}\right] + \frac{1}{2} \; Tr\left[\Sigma^{-1}(\boldsymbol{m}) \frac{\partial \Sigma(\boldsymbol{m})}{\partial m_i} \Sigma^{-1}(\boldsymbol{m}) \frac{\partial \Sigma(\boldsymbol{m})}{\partial m_j}\right] \quad (2)$$

where m_i is the thickness of the two basis materials, μ is the average of the measurements, and Σ is the covariance of the measurements. The measurements used here are the counts in the five bins.

The Cramer-Rao lower bound(CRLB) of the variance is the inverse of the Fisher information matrix. The CRLB provides a lower bound for the variance of the basis material estimates assuming that all deterministic errors can be corrected.

G. Imaging tasks:

A 120 kVp polychromatic spectrum with 10^6 photons/detector pixel and 2 cm of pre-patient aluminum filtration is transmitted through 2 cm of bone and different water thicknesses. Five energy bins with the following thresholds were selected {(1,38), (39, 52), (53, 60), (61, 77), (78, 120)} keV. We used these thresholds for the energy bins because they have approximately equal counts in the middle of the dynamic range of the absorber. Although photons below 20-30 keV are usually rejected in practice, a lower threshold for lowest energy bin was selected at 1 keV to capture multi-counting events.

A spectral imaging task is posed as estimation of water in projection space using material decomposition. Gaussian approximation of the Cramer-Rao Lower Bound (CRLB) of the water estimate using the three detectors' mean and covariance matrix estimates was used to compare spectral performance of different detectors.

III. RESULTS

A. Spatio-Energy Correlation

Figure 5 shows the correlation of energy bins of central pixel and the correlation of energy bins between central and neighboring pixels.

Figure 5 shows the correlation of energy bins of the central pixel and the correlation of energy bins between central and neighboring pixels. The covariance matrix is 5×5 because of the 5 energy bins of the detector. For a uniform central pixel illumination, the energy bins within each sub-pixel are independent, so the matrix is diagonal (Figure 5(a)), but the energy bins of the central pixels are correlated to energy bins of neighboring pixels (Figure5 (b)). Low energy bins of the central pixel are the most correlated energy, and are correlated in the decreasing order of the neighboring energy bin. Non-illuminated pixels have non-zero counts due to multi-counting events. By geometry, there are more counts in abutting pixels than in diagonal pixels. For uniformly illuminaion of all 9 pixels, there is stronger correlation between lower energy bins. Pixels that are not adjacent to each other do not have any correlation by assumption.

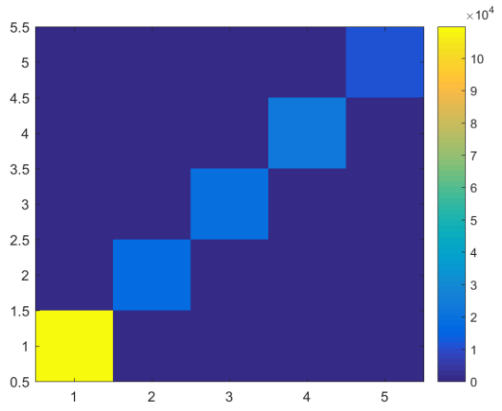

(a)

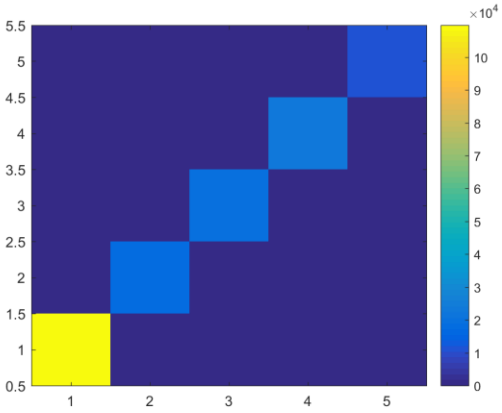

(b)

Figure 5: (a) covariance matrix of energy bins for central pixel, (b) covariance matrix of energy bins for central and neighboring pixel

B. Spectral Imaging Task Performance

We simulated uniform illumination of only the central pixel and also uniform illumination of all pixels. The results will be fully included in the presentation. Here we show some highlights. Figure 6 shows the CRLB of the variance of the water component fro all detector materials and also for an ideal detector (perfect energy response), for only central pixel illumination as well as for illumination of all pixels as a function of water thickness of the measured object. The increase with increasing thickness is simply due to lower photon flux with increasing thickness.

When only the central pixel is illuminated secondary photons and charge sharing cause degradation of the energy response but there is no overlap between true photon detection in one energy bin and secondary events photons detected in neighboring pixels. The degradation in the CRLB from this depends on the material and pixel geometry. It also depends on the object being measured since that affects the x-ray spectrum incident on the detector.

CdTe has high stopping power but suffers from escape of secondary photons, which tend to be low energy characteristic x-rays that can be absorbed in neighboring pixels or escape. CdTe also suffers from charge sharing. Both effects degrade the energy response function and cause correlations among neighboring pixels. While the central pixel illumination and all-pixel illiumination curves for Si and GaAs are virtually identical, the two curves for CdTe are different. This indicates that spatio-energy correlation effects degrade the performance of detector made by CdTe more than the other two materials (see Fig 6b). Si suffers from escape of Compton photons which are the largest source of energy response degradation in Si. These secondary photons are higher energy than the secondary photons in CdTe and can travel large distances (compared to the 0.5mm pixel size) and therefore are less likely to be detected in immediately neighboring pixels. Our simulations did not evaluate the impact of long distance correlations. The charge sharing of Si is the least of the three materials; accounting for charge sharing in Si makes no significant difference. GaAs shows the best performance according to our study (see Fig 6c) because it provides a good compromise of the flaws of Si and CdTe. In GaAs the secondary photons are also more likely to be reabsorbed in the same pixel and, like Si, it has little charge sharing.

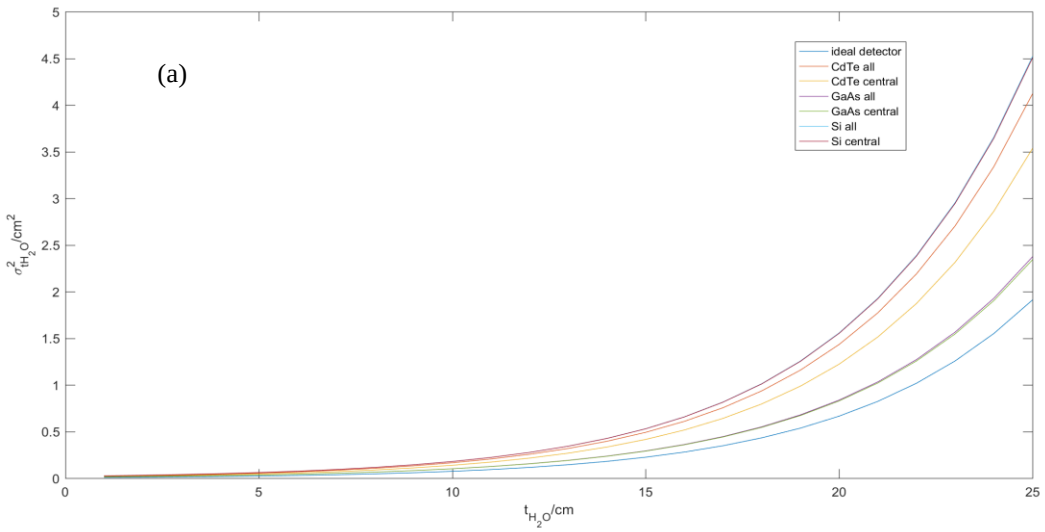

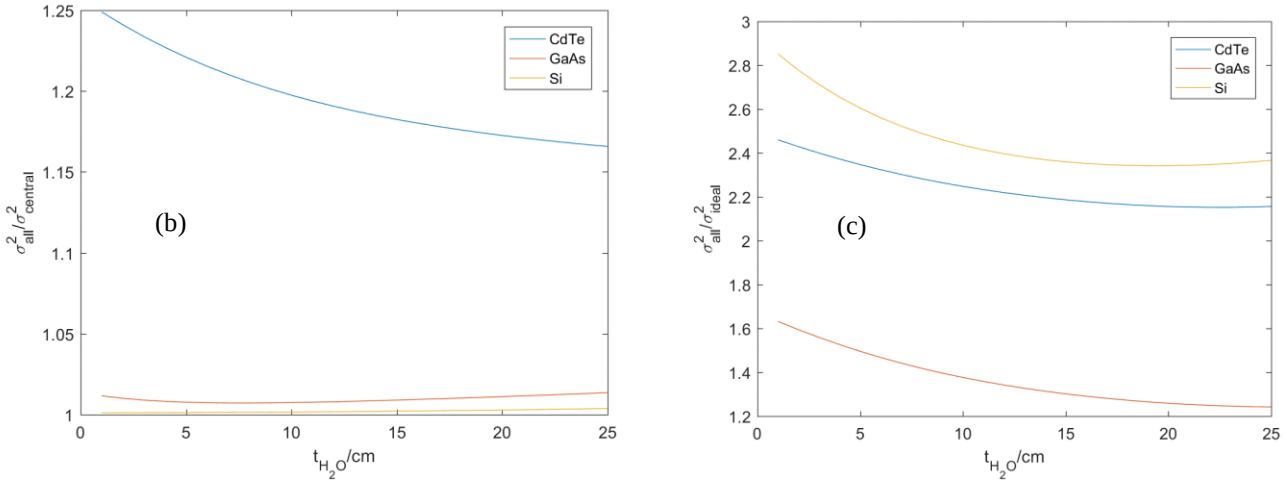

Figure 6: (a) the variance estimate in water with center illumination and all pixel illumination using three materials
(b) the ratio of the variance with all pixel illumination and center illumination of three materials
(c) the ratio of the variance with all pixel illumination and ideal detector of three materials

IV. CONCLUSION

CdTe (and CZT) and Si are both receiving significant attention as potential materials for PCDs for CT scanners. Our work suggests that detector materials whose atomic number is intermediate between CdTe and Si, such as GaAs, may also be a good candidate if practical but serious problems of availability and cost can be overcome. Future work could expand on the analysis of grey scale imaging performance, changing the size of sub-pixels, more accurate charge cloud models that are photon energy and absorption location dependent, and also pulse pile-up.

V. ACKNOWLEDGMENT

We thank Scott Hsieh for helpful discussions and Liu Bin for contributing to the calculation of Monte Carlo simulation.

REFERENCES

[1] Taguchi K, Iwanczyk J S. Vision 20/20: Single photon counting x-ray detectors in medical imaging[J]. Medical physics, 2013, 40(10).

[2] Taguchi, K., Polster, C., Lee, O., Kappler S.:Spatio-energetic cross-talks in photon counting detectors: detector model and correlated Poisson data generator," Proc. *SPIE Medical Imaging*, pp. 97831R-97831-9 (2016)

[3] Pautakh L. Rajbhandary, Scott S.Hsieh, Norbert J.Pelc: Effect of Spatio-energy Correlation in PCD due to charge sharing, scatter and secondary photons. *SPIE Medical Imaging*,(2017)

[4] Pinard, P. T., Demers, H., Salvat, F., Gauvin, R., pyPENELOPE Open Source. http://pypenelope.sourceforge.net/

[5] Kay SM. Fundamentals of statistical signal processing, volume 2: Detection theory. Prentice Hall PTR; 1998